Environmental niche variation and evolutionary diversification of the *Brachypodium distachyon* grass complex species in their native circum-Mediterranean range[1]

Diana López-Alvarez , Antonio J. Manzaneda , Pedro J. Rey , Patricia Giraldo , Elena Benavente , Joël Allainguillaume , Luis Mur , Ana L. Caicedo , Samuel P. Hazen , Adina Breiman , Smadar Ezrati , and Pilar Catalán

PREMISE OF THE STUDY: We conducted environmental niche modeling (ENM) of the *Brachypodium distachyon* s.l. complex, a model group of two diploid annual grasses (*B. distachyon*, *B. stacei*) and their derived allotetraploid (*B. hybridum*), native to the circum-Mediterranean region. We (1) investigated the ENMs of the three species in their native range based on present and past climate data; (2) identified potential overlapping niches of the diploids and their hybrid across four Quaternary windows; (3) tested whether speciation was associated with niche divergence/conservatism in the complex species; and (4) tested for the potential of the polyploid outperforming the diploids in the native range.

METHODS: Geo-referenced data, altitude, and 19 climatic variables were used to construct the ENMs. We used paleoclimate niche models to trace the potential existence of ancestral gene flow among the hybridizing species of the complex.

KEY RESULTS: *Brachypodium distachyon* grows in higher, cooler, and wetter places, *B. stacei* in lower, warmer, and drier places, and *B. hybridum* in places with intermediate climatic features. *Brachypodium hybridum* had the largest niche overlap with its parent niches, but a similar distribution range and niche breadth.

CONCLUSIONS: Each species had a unique environmental niche though there were multiple niche overlapping areas for the diploids across time, suggesting the potential existence of several hybrid zones during the Pleistocene and the Holocene. No evidence of niche divergence was found, suggesting that species diversification was not driven by ecological speciation but by evolutionary history, though it could be associated to distinct environmental adaptations.

KEY WORDS *Brachypodium distachyon*, *B. stacei*, *B. hybridum*; circum-Mediterranean native range; current and past bioclimatic envelopes; environmental niche modeling; model grasses; niche differentiation–conservatism; Poaceae; predicted distribution of potential hybrid zones

The characterization of areas where appropriate environmental conditions sustain the existence of a species is crucial for ecological, evolutionary, and conservation studies of organisms (Evans et al., 2009; Kirkpatrick and Barton, 1997). Niche modeling analyses and predictions of species distributions have been used for eco-biogeographic studies of plants and animals using environmental variables (Wollan et al., 2008; McCormack et al., 2010; Nakazato et al., 2010). These studies have been used to examine different ecological and evolutionary hypotheses, such as competition between phylogenetically related species (Anderson et al., 2002) or variation in species niche requirements through evolutionary time (Peterson and Holt, 2003; Peterson et al., 1999). They have further attracted interest in the dissection of potential adaptive speciation in plant species complexes where the distributions and interactions between diploid progenitors and their derived polyploids have both

overlapping and nonoverlapping ranges (McIntyre, 2012). The magnitude of environmental differentiation is critical to understand the origin and persistence of close diploid and polyploid species and the role of polyploidization in the evolution of ecological tolerances (Johnson et al., 2003).

Plant polyploids have been hypothesized to have broader niches than their diploid parents (Stebbins, 1971). Several studies have further indicated that polyploids occupy broader ecological distributions and could be more invasive than diploids due to their increased ecological amplitude (Meimberg et al., 2009; Pandit et al., 2011; te Beest et al., 2012). However, other studies have shown that the niche breadth of polyploids does not necessarily exceed that of their related diploids (Martin and Husband, 2009; McIntyre, 2012). Simple ecological models have suggested that niche differentiation is required for long-term coexistence of diploids and polyploids (Levin, 1975), but niche overlap is also frequent between diploids and polyploids and tends to be larger than between distinct diploids, probably as a consequence of the recent formation of (neo) polyploids with ecological amplitudes covering those of their diploid parents (Stebbins, 1971; Meyers and Levin, 2006).

The ecological properties of plant species and their ecological tolerances have a heritable component (Geber and Griffen, 2003). Environmental (ecological) niche modeling (ENM), also known as species distribution modeling (SDM) or predictive distribution modeling (sensu Graham et al., 2004; Peterson et al., 2007; Kozak et al., 2008), aims to identify the environmental conditions that characterize a species bioclimatic envelope (Nakazato et al., 2010). These models and their associated data can be used to test hypotheses about the environmental or evolutionary forces that might have shaped a species' geographic distribution and niche preferences (Graham et al., 2004). Spatially explicit environmental data and models allow for large-scale tests of whether speciation is associated with niche divergence or whether closely related species tend to be similar ecologically (niche conservatism) (McCormack et al., 2010).

Large-scale studies of angiosperms have shown that geographical ranges and environmental niche breadth are constrained by phylogenetic history, e.g., niche conservatism (Martin and Husband, 2009; Smith and Donoghue, 2010). Reconstruction of current and past environmental niches in the recent Pleistocene (e.g., Last Interglacial [LIG]; Last Glacial Maximum [LGM]) has helped us to understand the subsequent contractions and expansions of populations and to more accurately test for niche conservatism (Peterson and Nyari, 2008; Banks et al., 2008). Projections to these paleoenvironmental layers could also be used to search for potential niche overlap of parental diploids as a surrogate for detection of potential hybridization zones. This approach is of particular relevance in the circum-Mediterranean region, where altitudinal and latitudinal shifts and secondary contacts of previously isolated lineages were commonplace along the glacial and interglacial phases (Hewitt, 2004).

The "*B. distachyon*" complex is one of the most exhaustively studied world monocot groups because it is used as a research model for temperate cereals and biofuel grasses (Mur et al., 2011), for ecological studies of typical Mediterranean plants (Manzaneda et al., 2012), for the analysis of key physiological traits (e.g., drought tolerance, flowering time) (Gordon et al., 2014; A. J. Manzaneda, et al., University of Jaen, unpublished manuscript), and for the investigation of plant polyploid speciation (Catalán et al., 2014). The complex includes three related species, the diploids *B. distachyon* s.s. ($2n = 2x = 10$) and *B. stacei* ($2n = 2x = 20$), and their derived allotetraploid *B. hybridum* ($2n = 4x = 30$). Until recently, the three cytotypes were considered to be the same species, "*B. distachyon*", selected as a new model plant for functional genomics of grasses and monocots (Vogel et al., 2010; Catalán et al., 2014). However, combined cytogenetic and phylogenetic analysis demonstrated that *B. distachyon* and *B. stacei* corresponded to two independent diploid lineages and that *B. hybridum* resulted from genome doubling of the cross between them and probably originated in the mid-Pleistocene (ca. 1 Ma), supporting its species-level taxonomic differentiation (Catalán et al., 2012). The problems associated with the use of the collective name "*B. distachyon*"' (Catalán et al., 2012, 2014; López-Alvarez et al., 2012), precluded the use of the undetermined "*B. distachyon*" in Global Biodiversity Information Facility (GBIF) records in an ENM analysis. In this study, we investigated the spatial and temporal variation of environmental niches in the three circum-Mediterranean species of the *Brachypodium distachyon* s.l. grass ploidy complex, a noncrop model system of three annual plants with well-characterized genomes and geographic distribution (Vogel et al., 2010; Catalán et al., 2012; López-Alvarez et al., 2012).

The three species of the complex show a native geographic distribution that covers the entire circum-Mediterranean zone, (Schippmann, 1991; Garvin et al., 2008; Catalán et al., 2012). They grow in different environments, latitudes, and elevations, representing a wide range of biotic and abiotic conditions that may be associated with adaptive natural genetic variation (Garvin et al., 2008; Manzaneda et al., 2012). However, the specific distribution of each of the three species of the complex has still not been determined because most samples have been recorded under the collective name "*B. distachyon*".

We used environmental niche modeling (ENM) of the *B. distachyon* complex taxa to (1) construct the bioclimatic envelopes of the three species in their native range and identify the contributing variables using ENMs based on current geographic data and present and past climate data, (2) analyze niche overlap between the two diploids to detect potential hybridization zones across time, (3) test whether speciation in the *B. distachyon–B. stacei–B. hybridum* species was associated with niche divergence or responded to evolutionary history (niche conservatism), and (4) compare niche overlap and niche breadth between the diploid parents and the allotetraploid to test for potential outperforming of the polyploid in the native range. As a novel approach, our study uses paleoclimate niche models to corroborate the potential existence of ancestral gene flow among the hybridizing species of the *Brachypodium distachyon* model complex.

MATERIALS AND METHODS

***Study areas and data collection*—**Niche modeling analyses were conducted for each of the three species of the complex, the diploids *B. distachyon* s.s. ($2n = 2x = 10$; $x = 5$) and *B. stacei* ($2n = 2x = 20$; $x = 10$), and its derived allotetraploid *B. hybridum* ($2n = 4x = 30$; $x = 10 + 5$). Though the species can be differentiated morphologically (Catalán et al., 2012), they exhibit phenotypic resemblances in the field and are considered cryptic species. Therefore, despite the accumulation of more than 3175 circum-Mediterranean records of "*B. distachyon*" s.l. in the GBIF data repository, only records based upon specimens of *B. distachyon*, *B. stacei*, and *B. hybridum* identified

either cytogenetically by DAPI-stained chromosome counts (the three species; cf. López-Alvarez et al., 2012; this study) or by flow cytometry analysis (*B. hybridum* vs. diploids; cf. Catalán et al., 2012), or through species-specific DNA barcodes (the three species; cf. López-Alvarez et al., 2012; this study) or simple sequence repeat (SSR) markers (the three species; cf. Giraldo et al., 2012), were used. To the 210 samples (56 *B. distachyon*, 43 *B. stacei*, 111 *B. hybridum*) recorded in the study of López-Alvarez et al. (2012), we added 351 new records, totaling 561 accessions with locality data collected for *B. distachyon* (249), *B. stacei* (49), and *B. hybridum* (263) across their respective circum-Mediterranean native ranges (Fig. 2; Appendix S1, see Supplemental Data with the online version of this article). The sample size of *B. stacei* was smaller than those of *B. distachyon* and *B. hybridum*; however, this species is also the rarest of the three taxa (cf. Catalán et al., 2012; López-Alvarez et al., 2012), and its occurrence data are well represented with records spreading across its whole native circum-Mediterranean area (Fig. 2). *Brachypodium hybridum* occurrence data from noncircum-Mediterranean introduced populations (e.g., alien populations of central-western Europe, western North America, South America, South Africa, Australia, and New Zealand; cf. Bakker et al., 2009; Catalán et al., 2012; López-Alvarez et al., 2012) were not used in the analysis (see Discussion). The new accessions were obtained from our own field collections and from geo-referenced collections of "*B. distachyon*" s.l. obtained from herbaria and germplasm banks (Appendix S1). Procedures for DAPI-stained chromosome counts of germinated seeds and/or for DNA barcoding identification of leaf tissue of the new accessions followed those of López-Alvarez et al. (2012).

The GIS and environmental data for ENM analysis were preprocessed with the options implemented in the python version of the program SDMtoolbox (Brown, 2014). To correct the uneven sampling of the taxonomically identified *B. distachyon*, *B. stacei*, and *B. hybridum* accessions, we filtered the occurrence records to reduce the likely effects of spatial autocorrelation due to sampling bias. Filtering methods have been demonstrated to outperform unfiltered methods in correcting for sampling biases, which artificially increase spatial autocorrelation of the localities and may lead to overfit models with inflated values of performance (Boria et al., 2014). For this, we retained single-occurrence records of each of the three studied species in a range of 1 to 20 km, according to climate heterogeneity, using the Spatially Rarefy Occurrence Data tool implemented in SDMtoolbox v.1.1 in ArcGIS 10.1 by imposing five heterogeneity classes (Brown, 2014). Additionally, presence record bias was further addressed by creating a bias grid for use in Maxent (Brown, 2014). The bias grid was used to down-weight the importance of presence records from areas with more intense sampling (Elith et al., 2010) (i.e., areas with a high density of presence records, like Spain, Turkey, and Israel; Fig. 2; Appendix S1).

***Environmental niche modeling*—**Species distribution models of the three studied taxa were generated using the program Maxent v.3.3.3 (Phillips et al., 2006), which estimates the optimal potential distribution from a maximum entropy probability distribution from presence-only data (Elith et al., 2006; Araujo and Rahbek, 2006). Maxent has been found to perform better than other alternative modeling methods that are based on presence data alone (Elith et al., 2006; Ortega-Huerta and Peterson, 2008) and is particularly well suited for species with few data records (Hernandez et al., 2006; Pearson et al., 2007; Wisz et al., 2008; Benito et al., 2009). The environmental layers consisted of 19 temperature and precipitation Bioclim variables (Table 1), downloaded from the WorldClim data set (http://www.worldclim.org) (Appendix S2, see online Supplemental Data) and past climate reconstructions at a scale of 30 arc-seconds (ca. 1 km^2) for current, mid-Holocene (MH; ~6 ka) and Last interglacial (LIG; ~120–140 ka) scenarios, and 2.5 arc-minutes (c. 5 km^2) for Last Glacial Maximum (LGM; ~21 ka) scenarios (Hijmans et al., 2005b), plus altitude. These climatic niche variables describe environmental conditions rather than resources and are expected to show less spatial heterogeneity and higher correlations between close cells than ecological variables do (Soberón, 2010). However, ecological variables (e.g., soil, vegetation) are more difficult to measure over broad geographic areas (McCormack et al., 2010) or are less predictive than climate variables because their high variability at small GIS scales (Nakazato et al., 2010).

Current climatic data from each occurrence point were extracted using the program DIVA-GIS v7.5 (Hijmans et al., 2005a). To avoid overfitting of the data, we removed highly correlated variables ($R > 0.7$) and defined species-specific geographic backgrounds using the program SDMtoolbox v1.1. The estimated background areas of each species were generated using the buffered local adaptive convex-hull tool of SDMtoolbox v1.1, where each background area was intermediate between its larger buffered minimum convex polygon and its more restrictive radial distance area from all occurrence points. We imposed a buffer of 150 km, which fairly represents the potential dispersal distance of the three studied species (cf. López-Alvarez et al., 2012), and an alpha parameter value of 18, which depicts the search distance used to define the appropriate convex hull shape and size (Brown, 2014), around each set of locality data of *B. distachyon*, *B. stacei*, and *B. hybridum*.

The 19 bioclimatic variables were reduced to nine variables for *B. distachyon*, eight for *B. stacei*, and seven for *B. hybridum* (Table 1). The selected variables were used as predictors to calibrate the distribution models in Maxent. The occurrence data were randomly split into training (75%) and test (25%) data for model evaluation. Settings for the Maxent runs are given in the Supplemental Data (online Appendix S3). The performance of the models was evaluated by a threshold-independent Receiver-Operating Curve (ROC) analysis, where the Area Under the ROC Curve (AUC)—for Presence Only data (e.g., AUC-PO) measures the ability of the model to identify presences more accurately than random prediction. Ten subsample replicates were performed for each model using default settings. We used the average prediction from all the model replicates to construct the ENM species distribution maps. Additionally, a jackknife procedure was performed to measure the percentage of contribution and the importance of the variables to the models (Phillips et al., 2006).

The occurrence data of the three species under current conditions were projected to three past climatic envelopes to test the hypothesis of mid-Holocene and Pleistocene niche overlapping zones because the parental *B. distachyon* and *B. stacei* species might have favored the existence of putative hybrid zones across different temporal Quaternary windows, and to compare their potential niche overlap with the projected niche distribution of the allotetraploid *B. hybridum*. We used WorldClim past general circulation models (GCMs) to explore the potential variability of ENM scenarios during those periods. The Mid-Holocene (MH) envelope was simulated using the program Community Climate System Model version 4 (CCSM4) (Collins et al., 2006), the LGM paleoclimatic layers were simulated using three general atmospheric

circulation models—the Community Climate System Model version 4 (CCSM4) (Collins et al., 2006), the Model for Interdisciplinary Research on Climate (MIROC-ESM) (K-1 Model Developers, 2004), and the model of the Max Planck Institute for Meteorology (MPI-ESM-P) (Stevens et al., 2013), and the LIG envelope was simulated using the climatic model of Otto-Bliesner et al. (2006) (Appendix S2).

***Environmental niche comparisons and niche breadth*—**The niche comparison analyses from current data aimed to detect significant environmental differences among the three species for the 19 bioclimatic and three geographical (altitude, latitude, longitude) variables studied. This comparison was computed through one-way ANOVA tests and subsequent Tukey multiple comparisons test using the program Statistix v.8 (Analytical_Software, 2003). Additionally, a principal component analysis (PCA) of extracted data was also performed to discriminate the three species in the environmental space (Green, 1971; Austin and Smith, 1989) and to identify the variables that most contributed to their differentiation using the program Past v. 3 (Hammer et al., 2001).

The methods based on niche model comparisons included niche overlap analyses (niche identity, niche similarity) and niche breadth and were computed using the program ENMTools v1.4.2 (Warren et al., 2010). We quantified the amounts of niche overlap and niche breadth among the three studied species imposing a threshold of 10% of presence value for the occurrence of the taxon in a particular site, a method that shows accurate predictions when mapped with the program ArcGIS 10.1 (Raes et al., 2009). Given that each of the three species showed a different specific background area but with overlapping zones, we united them and created a common area to run the comparative niche pairwise tests and considered it as the study area. We performed niche comparisons across four temporal windows (current conditions, MH, LGM, LIG) for each species-pair and measured niche breadth for each separate species in each temporal scenario.

Pairwise niche overlap was assessed among the three species using Schoener's *D* metric (Schoener, 1968), which measures the proportional similarity of two distributions as an indicator of niche overlap. Test for niche differentiation was done through the niche identity test (or niche equivalence test), which tests the null hypothesis of niches being identical by randomly generating a distribution of niche overlap values with unknown species identities to which the observed overlap of Schoener's *D* is compared (Miller and Franklin, 2002; McIntyre, 2012). This is a one-tailed test, where niches are considered significantly different if the observed value of niche overlap is less than the niche overlap value from 95 ($P < 0.05$) or 99 ($P < 0.01$) of the niche overlap values estimated from the random pseudoreplicates.

The niche similarity test (or background similarity test) incorporates the environmental heterogeneity of the geographic ranges where the species occur and tests whether niche overlap is more or less similar than expected based solely on the regional environmental/background differences (null model) or to differences in niche suitability. A null distribution of overlap values was generated by comparing the species A niche model to a niche model created from a set of random points drawn from the species B background (with the same number of occurrences of A), and vice-versa. This process was repeated 100 times for each reciprocal comparison, generating a null distribution of 200 values for the Schoener's *D* for each species-pair. This is a two-tailed test, where the observed overlap values are then compared to these null distributions (Warren et al., 2008; McIntyre, 2012). According to Warren et al. (2008), rejection of the null hypothesis indicates that the niche models of two species are more different (overlap value < null distribution values) or more similar (overlap value > null distribution values) than would be expected by chance or that the observed niche differentiation between species is a function of habitat selection; however, failure to reject the null hypothesis does not necessarily imply that there is no niche differentiation or niche conservatism. By contrast, McCormack et al. (2010) used the niche similarity test based on niche models to test for niche divergence or conservatism, assuming that overlap values smaller than the null distribution support niche divergence (D), whereas larger values indicate niche conservatism (C). The niche similarity test is more relevant, regarding the speciation process, than the niche identity test (Smith and Donoghue, 2010); however, one critical aspect of the test is the circumscription of the background area. The background area of each species should be adjusted to the habitat available and should be biologically realistic (Warren et al., 2010). We chose as background areas the ENM of each species (Fig. 2) because they fit well the general dispersal abilities of these species (cf. López-Alvarez et al., 2012).

Niche breadth of a species is directly related to the extent of its geographic spread (Brown, 1984). We determined averaged niche breadth values for the three species under different climate scenarios (current climate, MH, LGM-CCSM4, LGM-MIROC, LGM-MPI-ESM-P, LIG). We used the suitability scores generated from each Maxent model, which were functions of specific environmental variables, to calculate Levin's concentration metrics, as implemented in ENMTools (Warren et al., 2010). Levin's concentration metric ranges from 0–1, where 0 indicates the minimum niche breadth when only one grid cell in the geographic space has a nonzero suitability and 1 indicates the maximum niche breadth when all grid cells are equally suitable (Mandle et al., 2010).

RESULTS

***Environmental variation of* B. distachyon, B. stacei, *and* B. hybridum—**Despite the apparent ecological uniformity of the "*B. distachyon*" s.l. complex taxa, we found fundamental environmental differentiation for its three species. Twelve of the 22 analyzed environmental (Bio1, Bio3, Bio4, Bio6, Bio7, Bio8, Bio10, Bio11, Bio12, Bio15, Bio17, Lat) variables detected significant differences ($P < 0.001$) among the three studied species (Table 1, Fig. 1A), and six (Bio2, Bio5, Bio9, Bio14, Bio18, Alt) between *B. distachyon* and *B. stacei–B. hybridum*, indicating that each species has unique ecological preferences. The most extreme environmental differences were found between *B. distachyon* and *B. stacei*; *B. hybridum* showed intermediate values between those of the two parental species for the 12 discriminant variables, including its intermediate location across the latitudinal gradient (Table 1, Fig. 1A).

The environmental space defined by the two first PCA axes showed a relative differentiation of the *B. distachyon* and *B. stacei* samples along the opposite extremes of the first axis (75.23% variance), whereas those of *B. hybridum* overlapped with both groups but more greatly with the *B. stacei* cluster (Fig. 1B). The variables that most contributed to the first PCA axes were altitude (PCA1), annual precipitation (PCA2) and temperature seasonality (PCA3) (online Appendix S4).

TABLE 1. Mean values of the 20 bioclimatic and altitudinal variables analyzed for environmental niche modeling of *Brachypodium distachyon*, *B. stacei*, and *B. hybridum* in their native circum-Mediterranean region. These variables plus latitude and longitude were used for comparative interspecific statistical analysis (22 variables).

		B. distachyon (*N* = 249)		*B. stacei* (*N* = 49)		*B. hybridum* (*N* = 263)		ANOVA
Enviromental variable	**Code**	**Mean**	**PC (PI)**	**Mean**	**PC (PI)**	**Mean**	**PC (PI)**	***F* (df)**
Annual mean temperature	Bio1	**12.6** ^{C}	**14.4 (10.2)**	**18.1** ^{A}	**0 (0.1)**	**16.3** ^{B}	**22.9 (25.1)**	**191 (2)** ***
Mean diurnal range	Bio2	**10.8** ^{A}	**2.1 (1.4)**	**10.0** ^{B}	**2.3 (0.2)**	**10.1** ^{B}	**31.1 (25.9)**	**9.64 (2)** ***
Isothermality	Bio3	**36.6** ^{C}	**15.2 (5.8)**	**40.3** ^{A}	**1.7 (2)**	**38.1** ^{B}	**11 (5.4)**	**29.6 (2)** ***
Temperature seasonality	Bio4	**690.3** ^{A}	**4.3 (6.6)**	**555.0** ^{C}	**44 (16)**	**607.2** ^{B}		**54.1 (2)** ***
Maximum temperature of warmest month	Bio5	29.1 ^{B}		31.4 ^{A}		31.1 ^{A}		**27.7 (2)** ***
Min temperature of coldest month	Bio6	−0.5 ^{C}		**6.6** ^{A}	**19.6 (24.8)**	4.4 ^{B}		**206 (2)** ***
Temperature annual range	Bio7	29.6 ^{A}		24.8 ^{C}		26.6 ^{B}		**40.7 (2)** ***
Mean temperature of wettest quarter	Bio8	**8.8** ^{C}	**5.5 (4.7)**	13.5 ^{A}		**11.9** ^{B}	**7.7 (8.2)**	**65.9 (2)** ***
Mean temperature of driest quarter	Bio9	**18.8** ^{B}	**10.5 (17.8)**	24.7 ^{A}		22.9 ^{A}		**46.1 (2)** ***
Mean temperature of warmest quarter	Bio10	21.2 ^{C}		25.0 ^{A}		24.0 ^{B}		**87.4 (2)** ***
Mean temperature of coldest quarter	Bio11	4.4 ^{C}		11.6 ^{A}		9.3 ^{B}		**240 (2)** ***
Annual precipitation	Bio12	**602.0** ^{A}	**24.1 (9.9)**	**481.7** ^{C}	**20.2 (52.5)**	**554.0** ^{B}	**19.3 (25.3)**	**11.1 (2)** ***
Precipitation of wettest month	Bio13	87.3		93.7		94.3		**2.12 (2) n.s.**
Precipitation of driest month	Bio14	**16.4** ^{A}	**17.5 (30)**	3.0 ^{B}		**6.5** ^{B}	**5.7 (1.8)**	**83.4 (2)** ***
Precipitation seasonality	Bio15	46.4 ^{C}		80.5 ^{A}		66.1 ^{B}		**68 (2)** ***
Precipitation of wettest quarter	Bio16	232.7		243.8		250.7		**1.89 (2) n.s.**
Precipitation of driest quarter	Bio17	65.4 ^{A}		**19.7** ^{C}	**7.5 (1.9)**	34.8 ^{B}		**62.9 (2)** ***
Precipitation of warmest quarter	Bio18	76.1 ^{A}		31.7 ^{B}		45.0 ^{B}		**45.5 (2)** ***
Precipitation of coldest quarter	Bio19	204.5		219.0		224.2		**2.02 (2) n.s.**
Altitude	Alt	**703.8** ^{A}	**6.4 (13.6)**	**268.7** ^{B}	**4.6 (2.5)**	**392.7** ^{B}	**2.3 (8.4)**	**42.2 (2)** ***
Latitude	Lat	39.7 ^{A}		34.9 ^{C}		37.2 ^{B}		**81.2 (2)** ***
Longitude	Lon	16.1 ^{A}		13.9 ^{AB}		10.1 ^{B}		**7.50 (2)** ***

Notes: Values of the variables selected to construct the environmental niche model (ENM) of each species with Maxent are in bold face. Superscripts letters denote Tukey pairwise comparisons among species; values with the same letter do not differ significantly ($P < 0.001$). PC and PI indicate estimates of percentage contribution and of permutation importance of the variables used in the ENM of each species, respectively. *N*, sample size. ANOVA, asterisks indicate significance level (***$P < 0.001$; n.s. nonsignificant).

The most influential variables on the ENMs were annual precipitation (24.1%) for *B. distachyon*, temperature seasonality (44%) for *B. stacei* and mean diurnal range (31.1%) for *B. hybridum* (Table 1, Fig. 1A). Further, the jackknife pseudoreplicate tests indicated that these variables showed the highest training gain when used in isolation for each of these species, while those which significantly decreased the gain of the model when omitted alone were precipitation of driest month and annual precipitation for *B. distachyon* and *B. stacei–B. hybridum*, respectively.

***Environmental niche models of* B. distachyon, B. stacei, *and* B. hybridum *under current climatic conditions*—**The environmental niche models of *B. distachyon, B. stacei*, and *B. hybridum* expanded along their entire native circum-Mediterranean region (Fig. 2; online Appendix S5). The respective niche distribution models showed high AUC-PO values (online Appendix S6) and included all the sampled localities of each species (Fig. 2A–C), supporting the high predictive power of these models. The predicted ENM of *B. distachyon* (Appendix S5) ranged from the Iberian Peninsula and Morocco in the west to northern Iran and southern Azerbaijan in the east, and from southern France in the north to the High Atlas (Morocco) and northern Israel in the south (Fig. 2A; online Appendix S7a), and that of *B. stacei* (Appendix S5) from the Canary Islands in the west to southeastern Iran in the east, and from northern Sardinia in the north to southwestern Morocco and southeastern Iran in the south (Fig. 2B, Appendix S7b). In contrast to the *B. distachyon* model, which showed a potential distribution of the species in higher altitudinal areas and more northern circum-Mediterranean latitudes, the *B. stacei* model predicted a distribution mostly circumscribed to coastal and lowland Mediterranean, Macaronesian and western Indian Ocean areas. The ENM of *B. hybridum* (Appendix S5) ranged from the Canary Islands in the west to Afghanistan in the east, and from southern France in the north to northwestern Sahara and southern Iran in the south (Fig. 2C; Appendix S7c). The predicted niche distribution of the allotetraploid covered both mountain and lowland and coastal circum-Mediterranean areas though was more common in the latter settings.

A comparative analysis of overlapping areas in the environmental niche distribution models of the three species detected ranges of potential shared occupancy between the two diploids (*B. distachyon* and *B. stacei*), the allopolyploid and both diploids (*B. hybridum* vs. *B. distachyon* and *B. stacei*), and the allopolyploid and one or the other diploid (Appendix S7d, e). The *B. distachyon* and *B. stacei* ENMs shared a distribution area (Appendix S5) that spread across the Iberian Peninsula, northwestern Africa, the Mediterranean islands, the Aegean region, and the Middle East (Appendix S7d). This area was similar in size and range to the geographic overlap detected for the ENMs of the three species (Appendices S5 and S7e). The ENM of *B. hybridum* overlapped with that of *B. distachyon* mostly in northwestern Mediterranean, southern France, and Caucasian localities, and with that of *B. stacei* in a greater area (Appendix S5) comprising localities mostly in the southern Mediterranean, Macaronesian, and Mediterranean islands (Appendix S7e). Additionally, the *B. distachyon* model showed a largest unique niche range, mostly distributed in northern Mediterranean latitudes, the *B. stacei* model the smallest one, mostly distributed in southern Mediterranean latitudes, and the *B. hybridum* model an intermediate size one, scattered across different localities in the whole region (Appendix S7e).

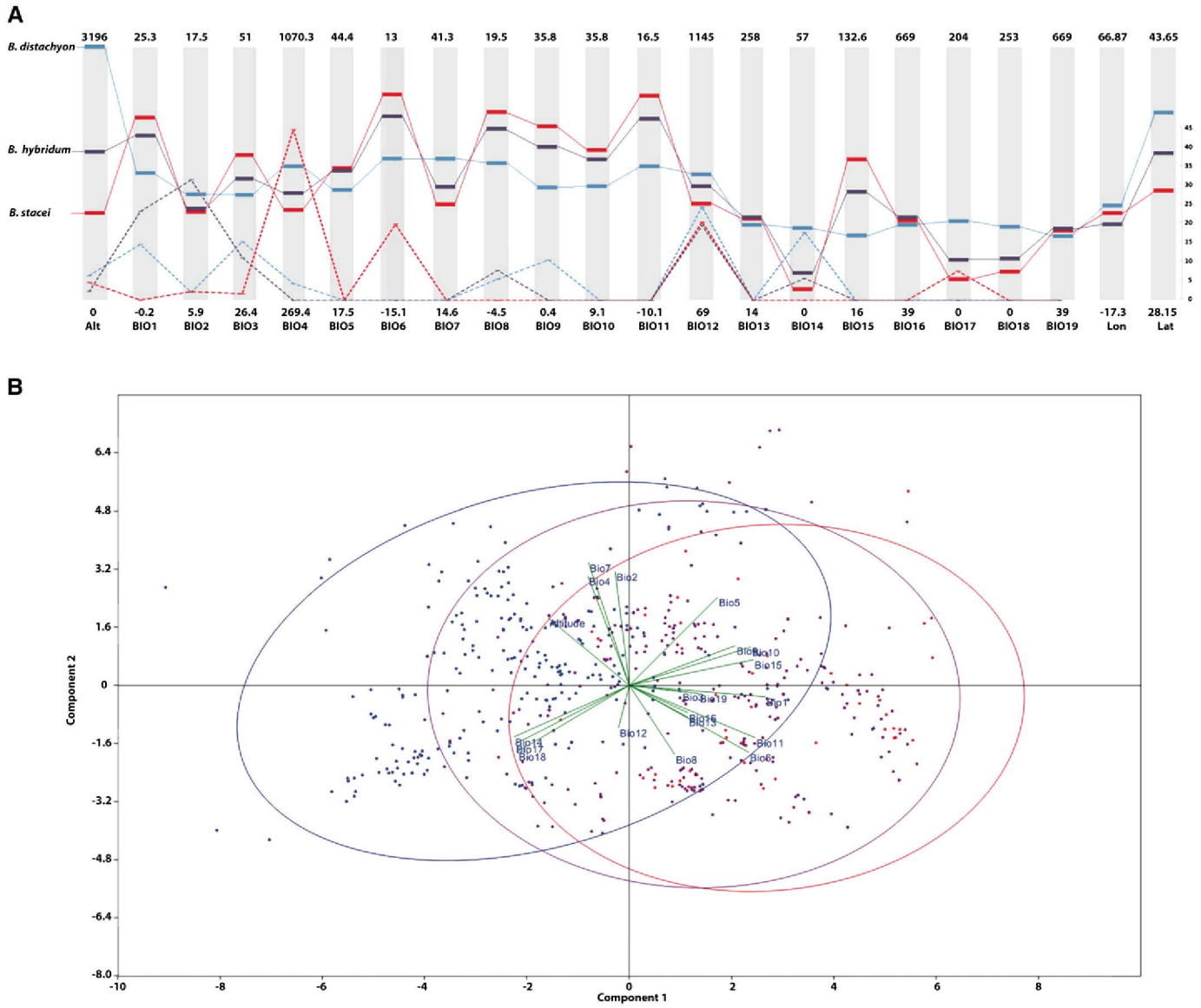

FIGURE 1 (A) Environmental variation of the *Brachypodium distachyon* complex species (*B. distachyon*, blue; *B. stacei*, red; *B. hybridum*, purple lines). Vertical bars represent the 19 climatic variables studied plus altitude, latitude, and longitude, with the species' mean values indicated by solid lines and the percentage contribution of each variable to the environmental niche model of each species (vertical scale on the right) represented by dashed lines. Numbers indicate the minimum and maximum values for each environmental variable. (B) Bidimensional principal component analysis (PCA) plot of *B. distachyon* (blue), *B. stacei* (red), and *B. hybridum* (purple) records based on data from 19 bioclimatic variables and altitude. PCA 1 and PCA 2 accounted for 75.23% and 17.30% of the variance, respectively (Appendix S4).

***Environmental niche models of* B. distachyon, B. stacei, *and* B. hybridum *under past climatic conditions*—**The projection of current presence data of *B. distachyon*, *B. stacei*, and *B. hybridum* to the MH, LGM, and LIG envelopes showed different temporal range shifts for their respective ENMs, though all of them supported the potential distribution of the three taxa in the circum-Mediterranean region (Figs. 3, 4; Appendices S8–S12). The MH environmental niche models of *B. distachyon*, *B. stacei* and *B. hybridum* (Appendix S8a–c) were not dramatically different from their respective ENMs under current climate conditions (Fig. 2A–C), sharing 82.2%, 54.4%, and 58.2% of their respective potential distribution areas (Appendix S5). Potential overlapped distributions of the species models in the MH decreased in all comparisons (*B. distachyon*–*B. stacei* 32.3%; *B. distachyon*–*B. hybridum* 32%; *B. stacei*–*B. hybridum* 49.8%; the three species 41.1%; Appendix S8d, e) with respect to the estimated overlaps of their current ENMs.

Of the three LGM environmental niche projections, we selected the projection based on the LGM-MIROC model (Fig. 3) as the optimal model because this climatic simulation provided a more convincing pattern of the LGM climate than the LGM-CCSM and LGM-MPI-ESM-P simulations (Tarkhnishvili et al., 2012). The LGM-CCSM model produced the most similar model distributions to the current climate model distributions of the three species, with percentages of niche model similarities of 80.9%, 97.3%, and 82.1% for *B. distachyon*, *B. stacei*, and *B. hybridum*, respectively (Appendices S5, S9a-c). The LGM-MPI-ESM-P model rendered ENMs

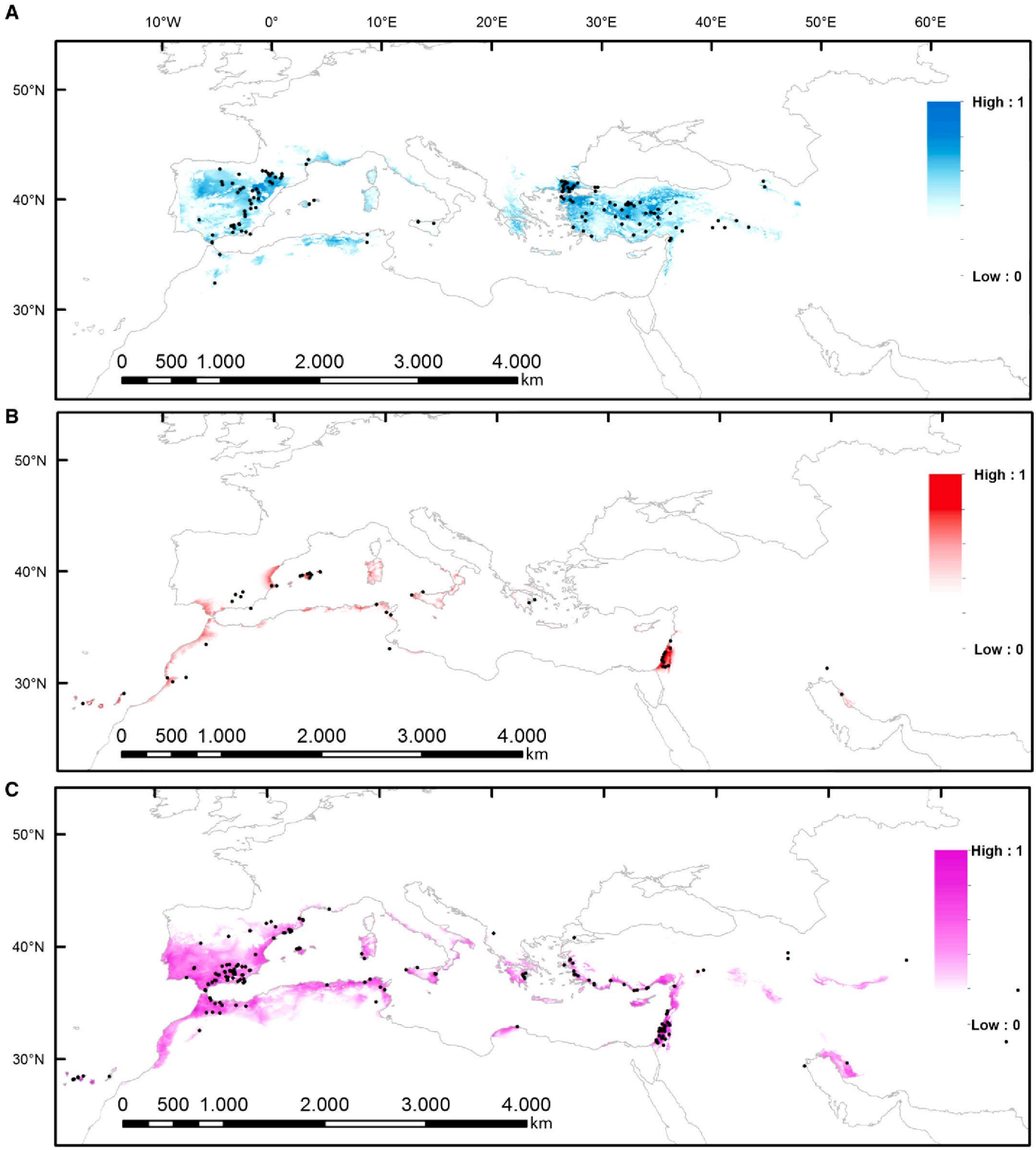

FIGURE 2 Summarized maps of ecological niche models constructed with Maxent for the three studied species in their native circum-Mediterranean range under current climatic conditions. (A) *Brachypodium distachyon* (blue). (B) *B. stacei* (red). (C) *B. hybridum* (purple). Scales indicate suitability scores. Dots correspond to occurrence data (see Appendix S1).

that slightly increased the niche distributions of *B. distachyon* (5.5%) and *B. stacei* (20.7%) and showed high similarity in geographic coverage for *B. hybridum* (81.3%) (Appendices S5, S10a-c) with respect to their current ENMs. The environmental niche projections of the LGM-MIROC model showed the highest increases in niche distributions for *B. distachyon* (44.5%) and

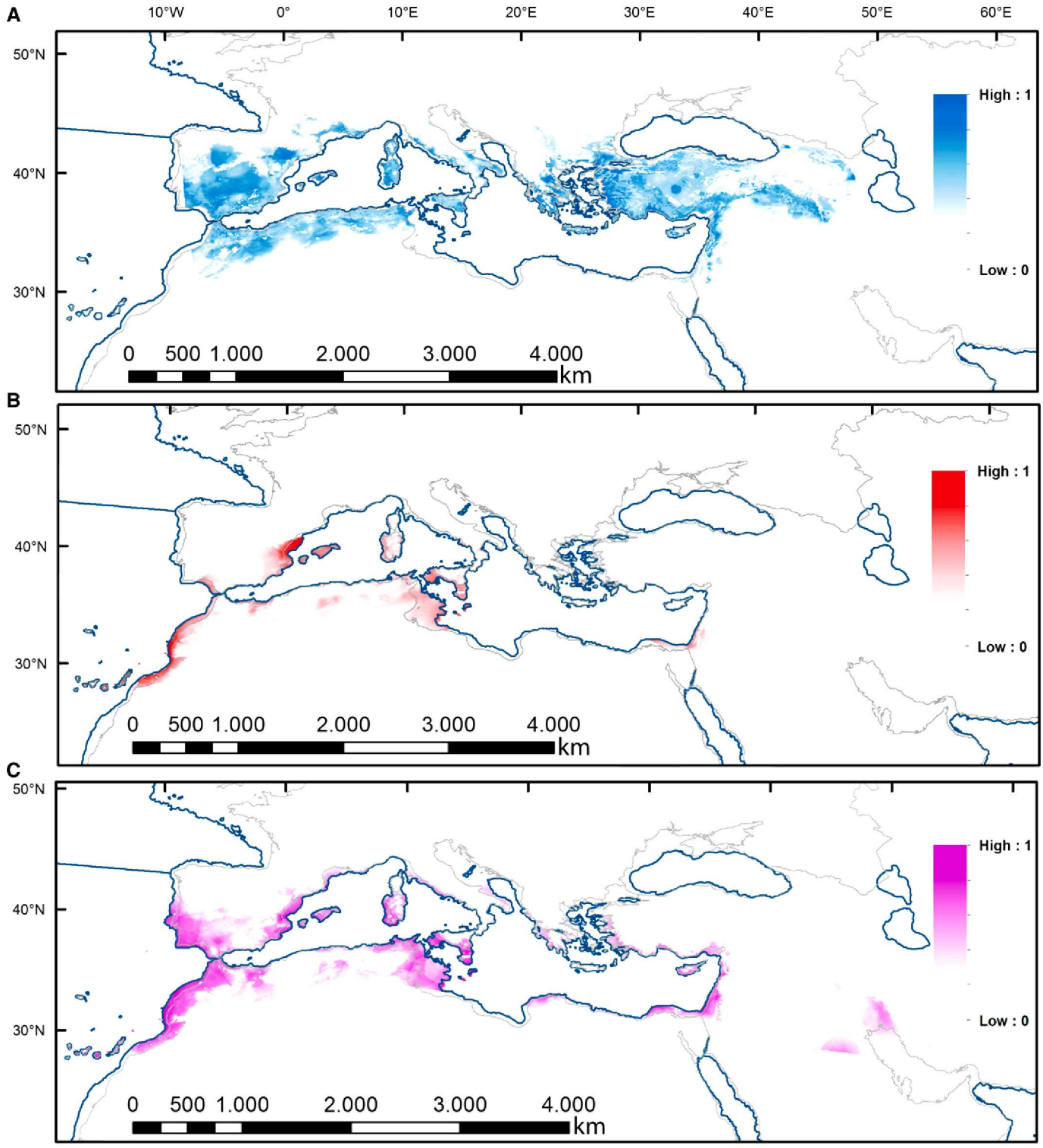

FIGURE 3 Summarized maps of ecological niche models constructed with Maxent for the three studied species in their native circum-Mediterranean range under Last Glacial Maximum (LGM) climatic conditions (MIROC model). (A) *Brachypodium distachyon* (blue). (B) *B. stacei* (red). (C) *B. hybridum* (purple). Scales indicate suitability scores. Blue line, 200 meters below sea level (mbsl).

B. hybridum (46.4%) and a small one for *B. stacei* (2.3%) (Fig. 3A–C; Appendices S5, S11a–c) regarding their respective present time projections. This increase may be inferred to have resulted from a shift to lower altitudinal areas (including a lowered coastal line of approx. 200 m below current sea level) and to a broader expansion to more southern and eastern circum-Mediterranean latitudes. All the ENMs of the three species showed an increase in all the LGM climatic models (Fig. 3A–C; Appendices S9a–c, S10a–c, S11a–c),

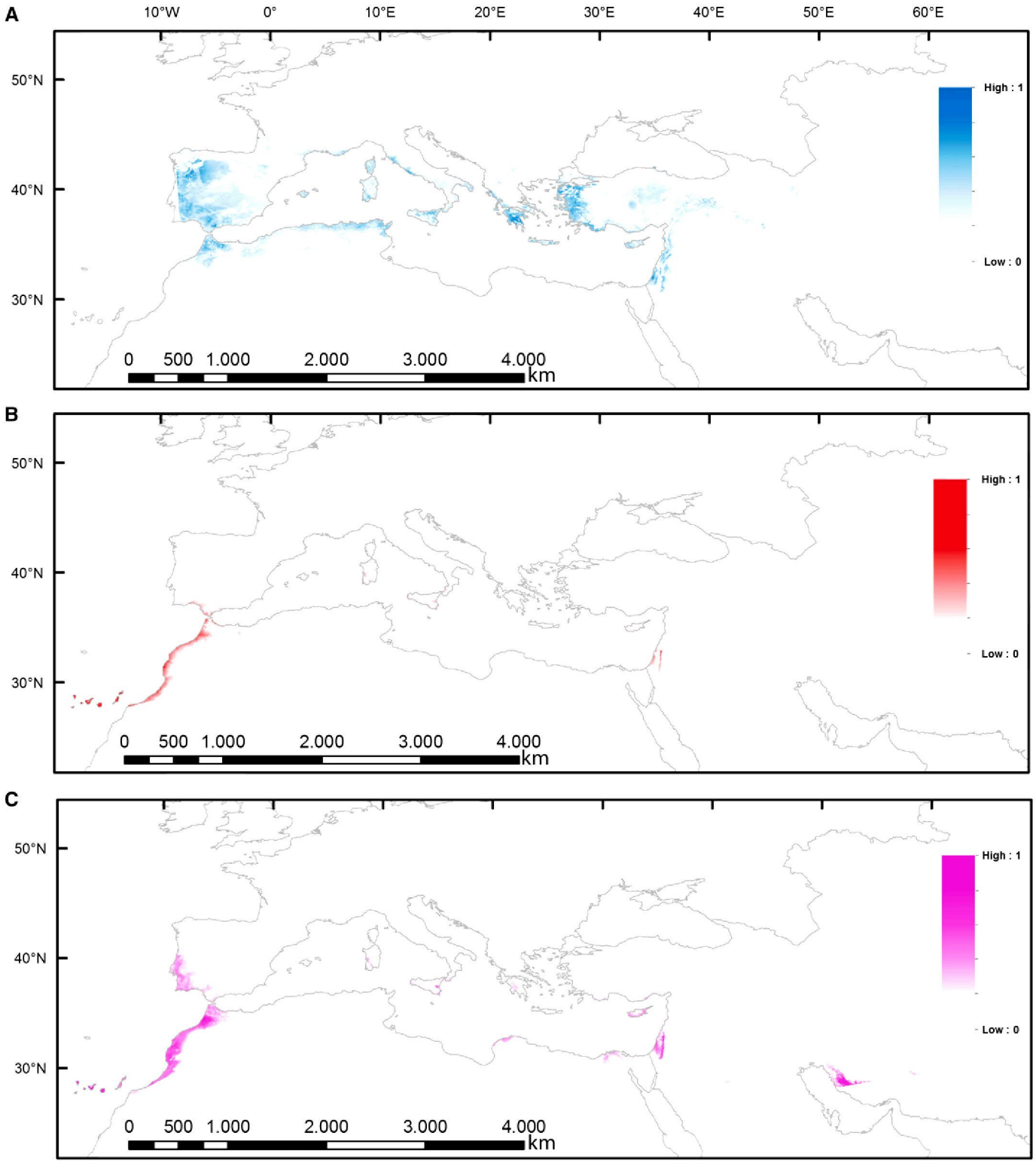

FIGURE 4 Summarized maps of ecological niche models constructed with Maxent for the three studied species in their native circum-Mediterranean range under Last Interglacial (LIG) climatic conditions. (A) *Brachypodium distachyon* (blue). (B) *B. stacei* (red). (c) *B. hybridum* (purple). Scales indicate suitability scores.

which could be explained by a larger potential expansion of the species on coastal and subcoastal areas along the Mediterranean and northern Africa. Consequently, the potential overlapped distributions of their respective past ENMs also increased in all LGM projections (*B. distachyon–B. stacei* 3.2% [CCSM], 97.7% [MIROC], 107% [MPI-ESM-P]; *B. distachyon–B. hybridum* 2.1% [CCSM], 98.8% [MIROC], 11.6% [MPI-ESM-P]; *B. stacei–B. hybridum* 15.6% [MIROC], 3% (MPI-ESM-P); the three species 2.7% [CCSM],

94.1% [MIROC], 71.3% [MPI-ESM-P]; Appendix S5) and were overall displaced to the south (Figs. 3A–C; Appendices S9a–c, S10a–c and S11a–c). The LGM models indicated a large overlap of distributions of the two diploids (Appendices S9d, S10d, and S11d) along with the polyploid (Appendices S9e, S10e, and S11e) in the Mediterranean islands, the half western Mediterranean side and several eastern Mediterranean and SW Asian settings.

In contrast to the MH and LGM projections, the environmental niche models obtained from the LIG (Fig. 4A–C) showed a decrease in potential distributions for the three species with respect to current potential distributions (Appendix S5). The *B. distachyon* ENM showed a 55.9% range contraction (Fig. 4A), especially in the mountains, with a potential range shift toward more coastal and western Mediterranean places, whereas the *B. stacei* and *B. hybridum* ENMs showed major reductions of 80% and 77.2% of potential range coverage, respectively (Fig. 4B, C). The ENMs of *B. stacei* and *B. hybridum* suggested that the species could be distributed along the southern coasts and islands of the Mediterranean basin, with higher probabilities in southwestern Mediterranean–Macaronesia and Middle East (Fig. 4B), and the Atlantic Mediterranean–Macaronesian front plus scattered spots across the remainder of the circum-Mediterranean region (Fig. 4C), respectively. The LIG models also reflected a decrease in the potential niche overlapped distributions of the taxa (Appendices S5 and S12d, e) with respect to current potential niche overlaps (*B. distachyon–B. stacei*, 78.3%; *B. distachyon–B. hybridum*, 81.4%; *B. stacei–B. hybridum*, 79.7%; the three species, 81%). Although the estimated overlapped ranges of the ENMs of the allotetraploid and its parents were mostly confined to the western Mediterranean–Macaronesian region (Appendix 12e), the overlapping distribution of the two diploids was spread across the Mediterranean basin (Appendix S12d).

***Equivalence, similarity, and breadth of the ENMs of* B. distachyon, B. stacei, *and* B. hybridum—**Niche overlap analysis under current climatic conditions in the native circum-Mediterranean region showed a pattern of low overlap for the ENMs of the two diploids ($D = 0.3629$) and a higher overlap for those of the allotetraploid *B. hybridum* and its parents, especially with *B. stacei* ($D = 0.7347$) and less with *B. distachyon* ($D = 0.4546$) (Table 2). The niche identity tests found significant environmental divergence in two species-pair comparisons, indicating that the niches of *B. distachyon* and *B. stacei* and *B. distachyon* and *B. hybridum* are different ($P < 0.01$), while the difference was not significant between the niches of *B. stacei* and *B. hybridum* (Table 2). However, pairwise comparisons from the reciprocal niche similarity tests indicated that there were no significant differences in any case ($P > 0.05$; Table 2), suggesting that the observed niche differentiations have not been driven by ecological selection. Nonetheless, the observed values of overlap were larger than the null distributions of background divergence in some comparisons (Fig. 5, Table 2), suggesting niche conservatism for *B. distachyon* vs. *B. hybridum* (Fig. 5B) and especially for *B. stacei* vs. *B. hybridum* (Fig. 5C, Table 2).

The patterns of niche overlap among the three species under past climatic scenarios were, in general, highly congruent with the

TABLE 2. Observed niche overlap values and results of tests of niche equivalency (Identity test) and niche similarity (Background test) for different taxonomic and temporal (Current, Mid-Holocene, Last Glacial Maximum [LGM], and Last Interglacial [LIG] climatic conditions) species-pair comparisons. Background tests were conducted only under current climate conditions. The observed and simulated overlap values are based on Schoener's *D* metric. In the background similarity test the values correspond to the estimated niche overlap within a species pair when the occurrence data of the first species listed in the column (A) is projected into the niche distribution of the second species (B) and vice versa.

			Background test	
Species pair (A–B)	**Observed overlap**	**Identity test**	**A vs. B**	**B vs. A**
Current climate				
B. distachyon–B. stacei	0.3629	0.4051** D	0.3383^{ns} NC	0.2560^{ns} NC
B. distachyon–B. hybridum	0.4546	0.7087** D	0.3289^{ns} C	0.3098^{ns} C
B. stacei–B. hybridum	0.7347	0.6479^{ns}	0.2648^{ns} C	0.3051^{ns} C
Mid-Holocene (CCSM4)				
B. distachyon–B. stacei	0.2484	0.7060** D	—	—
B. distachyon–B. hybridum	0.4039	0.7515** D	—	—
B. stacei–B. hybridum	0.6299	0.6511** D	—	—
LGM (CCSM4)				
B. distachyon–B. stacei	0.4392	0.7085** D	—	—
B. distachyon–B. hybridum	0.4964	0.7328** D	—	—
B. stacei–B. hybridum	0.7875	0.6524** D	—	—
LGM (MIROC)				
B. distachyon–B. stacei	0.3788	0.7085** D	—	—
B. distachyon–B. hybridum	0.4574	0.7328** D	—	—
B. stacei–B. hybridum	0.6775	0.6524** D	—	—
LGM (MPI-ESM-P)				
B. distachyon–B. stacei	0.4261	0.7085** D	—	—
B. distachyon–B. hybridum	0.3771	0.7328** D	—	—
B. stacei–B. hybridum	0.7099	0.6524** D	—	—
LIG				
B. distachyon–B. stacei	0.1513	0.7085** D	—	—
B. distachyon–B. hybridum	0.1595	0.7328** D	—	—
B. stacei–B. hybridum	0.5468	0.6524** D	—	—

Notes: Overlap values smaller that the null distribution support niche divergence (D) and values larger than it niche conservatism (C); when niche overlap values are similar to the null distribution background the results are inconclusive (NC). Asterisks denote significance at $*P < 0.05$ and $**P < 0.01$; ns, nonsignificant.

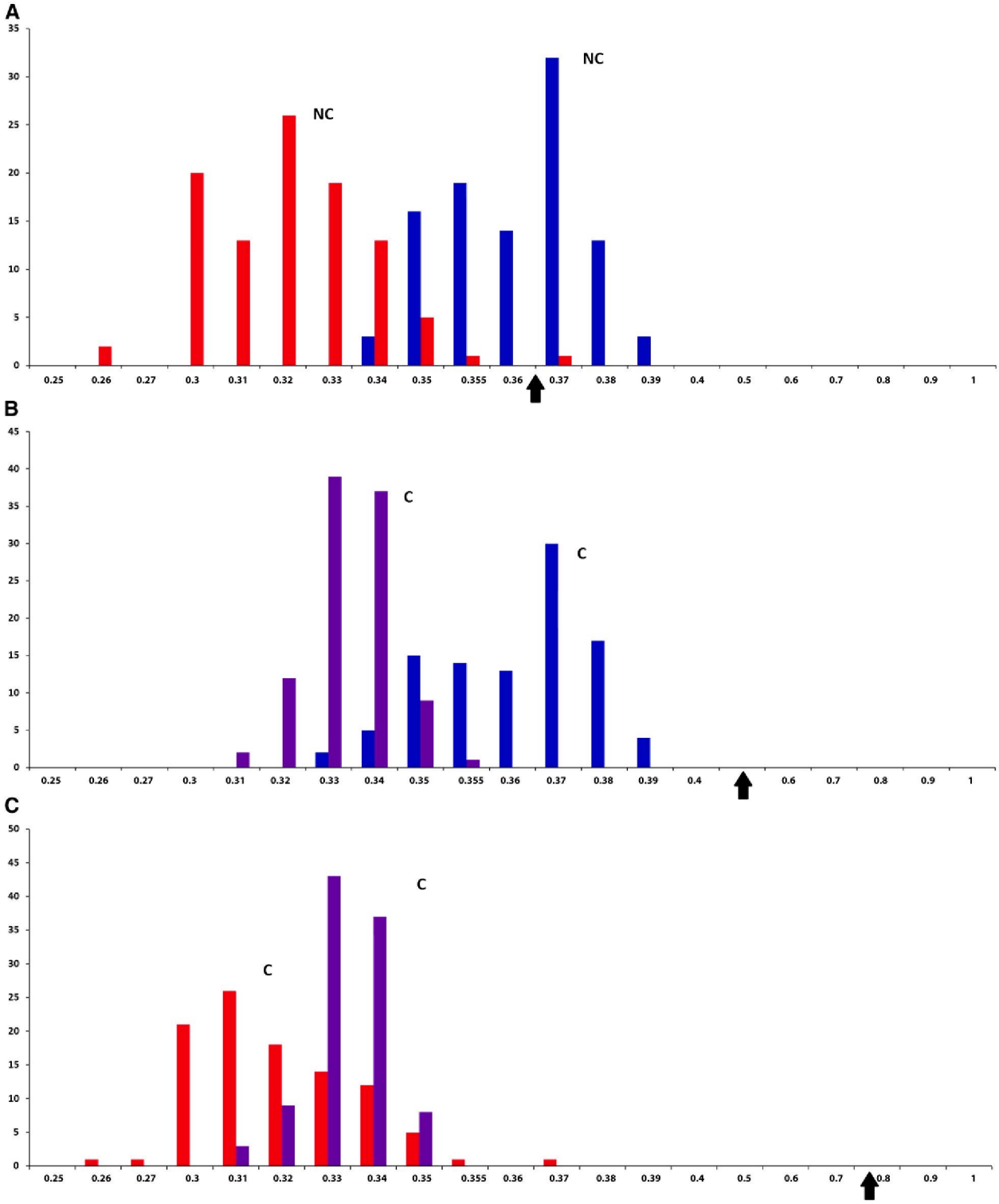

FIGURE 5 Plots of niche divergence and conservatism tests from environmental niche models of *Brachypodium distachyon* (blue), *B. stacei* (red), and *B. hybridum* (purple). Niche overlap values (arrows) were compared to two reciprocal null distributions of background divergence for each species pair (see text). Overlap values smaller or larger than the null distribution support niche divergence (D) and niche conservatism (C), respectively; results are inconclusive (NC) when the niche overlap value is similar to the null distribution background.

current models (Table 2). The *B. distachyon* and *B. stacei* niches showed a low overlap in the MH (D = 0.2484) and the LIG (D = 0.1513), and a relatively high overlap in all the LGM cases (D = 0.4392, LGM-CCSM4; 0.3788, LGM-MIROC; 0.4261, LGM-MPI-ESM-P). The *B. hybridum* niche showed a higher overlap with the *B. stacei* niche (D_{MH} = 0.62998; $D_{LGM\text{-}CCSM4}$ = 0.7875;

$D_{LGM\text{-}MIROC}$ = 0.6775; $D_{LGM\text{-}MPI}$ = 0.7099; D_{LIG} = 0.5468), than with the *B. distachyon* niche (D_{MH} = 0.4039; $D_{LGM\text{-}CCSM4}$ = 0.4964; $D_{LGM\text{-}MIROC}$ = 0.4577; $D_{LGM\text{-}MPI}$ = 0.3771; D_{LIG} = 0.1595) across all temporal windows (Table 2). Niche identity tests for past ENMs retrieved significant differences in niche equivalence for each separate pairwise species comparison in the MH, LGM and LIG scenarios.

Observed niche breadth of the three species in their current native range was greater for *B. distachyon* (0.2637) than for *B. hybridum* (0.1956) or *B. stacei* (0.1829), the latter species having the narrowest niche breadth value (Table 3). Similar results were observed for values of the three taxa in the past MH, LGM, and LIG scenarios, with *B. distachyon* having even broader niches in the LGM (MIROC and MPI-ESM-P models) and the three species having narrower niches in the LIG. *Brachypodium stacei* only had a slightly broader niche than *B. hybridum* in the LGM-MIP-ESM-P scenario (Table 3).

DISCUSSION

***Niche differentiation vs. conservatism suggests distinct environmental adaptations of* B. distachyon *and* B. stacei *and shared niche occupancy of* B. hybridum *with its parents in the circum-Mediterranean region*—**Environmental niche modeling approaches can detect divergence in adaptation to different ecological niches between candidate species and can also provide evidence on the type of speciation involved (Graham et al., 2004; Raxworthy et al., 2007; McCormack et al., 2010; Nakazato et al., 2010; Oliver and Ruiz-Rejon, 1980). Temperature and precipitation are the most important factors that determine the geographical distribution and abundance of plant species (Woodward, 1988), allowing each species to maintain populations in a specific geographical area, known as the fundamental niche (Hutchinson, 1957). However, bioclimatic variables are commonly used to build the environmental climatic niche (also called Grinellian or realized niche; Soberón, 2010; Jaime et al., 2015), since the fundamental (or Eltonian) niche should include many more abiotic and biotic (resource) variables (Soberón, 2010; Peterson, 2011; Araujo and Rahbek, 2006). Nonetheless, bioclimatic variables have shown a higher niche predictive power than other resource variables over large geographical areas (Nakazato et al., 2010), and their intrinsic spatial autocorrelation problems are less acute when analyzing species with sympatric distributions (McCormack et al., 2010).

TABLE 3. Averaged estimates of niche breadth, based on Levin's concentration metrics, for the species of the *Brachypodium distachyon* s.l. complex in their native circum-Mediterranean region at different temporal slices (Current, Mid-Holocene, Last Glacial Maximum, and Last Interglacial climatic conditions).

Species	Average niche breadth
Current	
B. distachyon	0.2637
B. stacei	0.1829
B. hybridum	0.1956
Mid Holocene (CCSM4)	
B. distachyon	0.2278
B. stacei	0.1298
B. hybridum	0.1697
Last Glacial Maximum (CCSM4)	
B. distachyon	0.250
B. stacei	0.111
B. hybridum	0.195
Last Glacial Maximum (MIROC)	
B. distachyon	0.412
B. stacei	0.180
B. hybridum	0.250
Last Glacial Maximum (MPI-ESM-P)	
B. distachyon	0.276
B. stacei	0.146
B. hybridum	0.130
Last Interglacial	
B. distachyon	0.2175
B. stacei	0.1120
B. hybridum	0.1458

Consistent with their nonmonophyletic, reticulate nature (Catalán et al., 2012, 2014), *B. distachyon*, *B. stacei*, and *B. hybridum* show overlapping distributions in the circum-Mediterranean region (Fig. 2; Appendix S7) and sympatric admixed populations (*B. distachyon–B. hybridum*, *B. stacei–B. hybridum*, and the three species) in several localities (Appendix S1). Our study has provided the first testable results on the environmental differentiation of the three annual species in their native range. Furthermore, our data also support balanced niche distribution coverages between the diploids and the allotetraploid in the native region but with distinct niche breadths.

The statistical and niche identity test analyses conducted show a clear differentiation of the environmental niches of *B. distachyon* and *B. stacei* (Tables 1, 2; Fig. 2A, B; Appendix S7a. b). The *B. hybridum* ENM mostly overlaps with those of one or the other parental species (Fig. 2); however, it is also characterized by specific environmental traits, usually intermediate between those of its progenitors, that significantly discriminate it from the others (Table 1) and that support its own realized niche (Fig. 2C; Appendix 7c). The environmental data indicate that *B. distachyon* grows in higher, cooler, and wetter places than *B. stacei*, which grows in lower, warmer, and drier environments, whereas *B. hybridum* grows in zones with intermediate values but also in low-altitudinal, warmer, and drier places, like its *B. stacei* progenitor (Tables 1, 2; Fig. 2C; Appendix S7c). These results fit well the ecophysiological requirements of the species (e.g., vernalization for most of the *B. distachyon* accesions and lack of it for the *B. hybridum* and *B. stacei* accessions; cf. Vogel et al., 2009; D. López-Alvarez and P. Catalán, unpublished data), which are crucial for the germination of seeds (Atwell et al., 1999; Vogel et al., 2009) and survival of these annual species in their respective Mediterranean niches. They also agree with Manzaneda et al. (2012), who found a north vs. south geographical structure for *B. distachyon* and *B. hybridum* associated with increasing aridity clines in the Iberian Peninsula. The discrimination of the three species across a latitudinal gradient in the study area (Table 1), remarkably reflects the latitudinal distribution of the present Mediterranean microclimes and explains the scarcity of *B. distachyon* occurrences and predicted niche in the south (restricted to high elevations) and the absence of *B. stacei* in the north (Fig. 2).

The amount of significant environmental differences found between *B. distachyon* and *B. stacei* for 18 environmental variables (Table 1, Fig. 1A) and combined PCA (Fig. 1B), and their divergence in niche equivalence (Table 2) suggest distinct adaptations to different ecological tolerances in these diploids. However, the reciprocal niche similarity tests were nonsignificant in both directions (Table 2, $P > 0.05$; Fig. 5A), implying that niche divergence was not the major driver of speciation for these species. By contrast, the pairwise comparison tests showed evidence of niche conservatism for *B. hybridum* and each of its parents (Fig. 5B, C). Phylogenetic

niche conservatism theory predicts that niches are conserved over evolutionary time due to selection pressure (Peterson et al., 1999) and that lineage splitting is not accompanied by relevant niche differentiation (Rundell and Price, 2009) but rather by reproductive isolation (McCormack et al., 2010) or other biological or life-history traits (Warren et al., 2008). Most evolutionary ecological studies conducted with sister lineages have accumulated evidences of niche conservatism (Wiens and Graham, 2005; Warren et al., 2008); but niche conservatism has been also found across non-related lineages (Warren et al., 2008; Peterson, 2011). In our case, niche conservatism is predicted for the recent allopolyploid, which shares niche occupancy with both progenitors but is reproductively isolated from them.

Our phylogenetic studies have demonstrated that the two morphologically close parental species correspond to two highly divergent lineages of which *B. stacei* split first from the common ancestor in late Miocene times (stem age ~9.9 Ma), whereas *B. distachyon* split more recently in near Pliocene times (stem age ~4.3 Ma) (Catalán et al., 2012). The evolutionary and environmental niche data suggest that the more recently evolved *B. distachyon* could have adapted to different environmental conditions than the more ancestral *B. stacei*. It could be hypothesized that the ancestor of *B. stacei* speciated by adaptation to aridic Messinian conditions, whereas *B. distachyon* did to more mesic conditions at the onset of the Mediterranean climate. Their ecological divergence is also reflected in their different niche breadths, with *B. distachyon* showing higher levels of heterogeneous environmental variability than *B. stacei* (Table 3).

Niche overlap of diploid parents supports multiple potential hybrid zones across past scenarios—Reconstruction of past climate envelopes (MH, LIG, LGM) of *B. distachyon*, *B. stacei*, and *B. hybridum* have provided testable scenarios about their predicted range shifts and their subsequent niche overlapping areas (Figs. 3, 4; Appendices S8–S12). One of the most noticeable findings was the larger geographical niche distributions that the three species showed in the LGM (Fig. 3; Appendices S9, S10) compared with the current distributions (Fig. 2). Environmental niche studies of Holarctic plants and animals usually predict range contractions or fragmentations in the LGM due to unfavorable climatic conditions (Waltari et al., 2007; Stewart et al., 2010); however, several cases of range expansion have been proposed depending on the climatic tolerance of the species, the size and environmental suitability of the new ranges and the existence of both latitudinal and longitudinal refugia (Stewart et al., 2010) in either lowland and alpine-montane plants (Fernández-Mazuecos and Vargas, 2013; Russell et al., 2014). Our results are consistent with the hypothesis of circum-Mediterranean peninsulas and islands as major warm refugia for plants during the last glacial phases (Médail and Diadema, 2009; Feliner, 2011). These refugia, coupled with the dropping of sea level ca. 150 m (Lambeck and Chappell, 2001; Lambeck et al., 2002; Clark and Mix, 2002), likely favored the latitudinal range shifts and the increased niche distribution ranges predicted for these annual species in the LGM (Fig. 3). Conversely, a trend toward range contraction was reconstructed for the niche models of the three species in the LIG (Fig. 4), though the three paleoniche models mostly fit the current distribution ranges of the species. Our ENM study supports the Mediterranean basin and its adjacent areas as "long-term refugia" (Stewart et al., 2010) for *B. distachyon*, *B. stacei*, and *B. hybridum*, showing that these zones likely ensured the long-term persistence of their populations through the last glacial cycle (Fernández-Mazuecos and Vargas, 2013).

The paleoclimatic MH, LGM, and LIG models provided further insights about the potential overlapping of environmental niches of the two diploid parents and its hybrid. A larger and a more restricted potential range overlap was predicted for *B. distachyon* and *B. stacei* in the LGM and the MH and LIG, respectively (Appendices S8d–S12d). Interestingly, both ranges were distributed across the southern Mediterranean basin and its islands (Appendix S7d). Our paleoenvironmental MH/LGM/LIG and current niche models support the occurrence of potential areas of niche overlap between the two diploid parents across Mid-Holocene and Pleistocene time, which might have favored the existence of multiple potential hybrid zones along their native Mediterranean basin. This concurs with the hypothesis of the recurrent and polytopic origin of the allopolyploid *B. hybridum* in the circum-Mediterranean area from distinct bidirectional crosses of alternative maternal and paternal *B. stacei*/*B. distachyon* progenitors, deduced from analysis of plastid and nuclear barcode DNA sequences in the three species (López-Alvarez et al., 2012).

Despite genetic studies confirming long-distance dispersal of genotypes of these species in the Mediterranean region (Catalán et al., 2012; López-Alvarez et al., 2012), López-Alvarez et al. (2012) detected signatures of geographical structure on both sides of the circum-Mediterranean area, with unique *B. hybridum* genotypes coinherited from their respective western and eastern Mediterranean parental *B. distachyon* and *B. stacei* genotypes. The selfing nature of the three reproductively isolated species (Mur et al., 2011; Catalán et al., 2012) and the current cytogenetic stability of the *B. hybridum* individuals ($2n = 30$ chromosomes; López-Alvarez et al., 2012; present study) further support the multiple polyphyletic origin of the allotetraploid in the past (López-Alvarez et al., 2012). Recurrent origins of allopolyploid plants have been widely described (Soltis and Soltis, 1999; Meimberg et al., 2009; Estep et al., 2014), but few studies have investigated its potential occurrence across past scenarios. Our study provides evidence based on an environmental model for the plausible occurrence of *B. distachyon* and *B. stacei* niche overlap and subsequent hybrid zones in their native range across different mid-Holocene and Pleistocene temporal scenarios where the hybrid presence has been also predicted (Fig. 2; Appendices S7, S12).

The allopolyploid does not outperform its diploid parents in their native range—Our study indicates that though *B. hybridum* has a unique environmental niche, which is significantly different at least from that of *B. distachyon* (e.g., niche equivalence test, Table 2) and presents significant differences with its parents in 12 bioclimatic variables (Table 1), it has a smaller niche distribution than that of *B. distachyon* (Table 3) and overlaps greatly with the niches of the two diploids, especially with that of *B. stacei* (Appendix S7). Niche similarity analyses were inconclusive regarding the potential divergence of the *B. hybridum* niche with respect to those of *B. distachyon* and *B. stacei* (Table 2), though reciprocal background distribution tests supported niche conservatism for *B. hybridum* and both progenitors (Fig. 5B, C). Several environmental studies of plants have shown that different ploidy taxa occupy different niche environments and ecologically diverge from one another (Buggs and Pannell, 2007; McIntyre, 2012). However, other studies have detected both separate niches and also different ploidies coexisting in the same area (Oliver and Ruiz-Rejon, 1980) or geographically separated diploid and polyploid ranges but with polyploids occupying environmental

niches that are predicted to be suitable to diploids (Godsoe et al., 2013). We found that the three species of the *B. distachyon* complex could potentially coexist in an area of 260 119 km^2 (Appendix S5), though each separate species or combinations of species-pairs showed larger niche distribution ranges depending on the environmental requirements of each species (Appendix S7).

Allopolyploids that combine the genomes and phenotypic characteristics of diploids can exhibit a greater degree of niche overlap (Miller and Franklin, 2002; McIntyre, 2012) and consequently might show an increased range of phenotypic responses resulting in their often reported broader environmental tolerances relative to diploids (Levin, 1983). Interestingly, *B. hybridum* had the largest niche overlap compared with its two diploid progenitors, being phenotypically more variable (Catalán et al., 2012; D. López-Álvarez and P. Catalán, unpublished data) but a niche breadth smaller than that of *B. distachyon* and only slightly greater than that of *B. stacei* (Table 3). Niche competition with its diploid progenitors could be invoked to explain the observed restricted range distribution and niche breadth of *B. hybridum* in its native area, overlapping with but not displacing them.

Conversely, *B. hybridum* is the only species of the complex that has apparently successfully colonized other nonnative world regions for which confirmed GIS occurrence data are still scarce (e.g., Central Europe, North America (California), South America (Uruguay), South Africa, Australia, New Zealand; cf. Jenkins et al., 2003; Garvin et al., 2008; Bakker et al., 2009; Catalán et al., 2012). The fact that the new noncircum-Mediterranean environments were only colonized by *B. hybridum* but not by its parents, assuming similar chances of man-mediated seed introduction for the three cryptic annual species, suggests a greater ecological tolerance of the allotetraploid compared with the diploids and its high capability to adaptation to climatically similar territories but where the parental diploids are absent. This possibility could be explained by the high potential of highly heterozygous allopolyploids to large genome rearrangements and to genomic and epigenetic expressions, increasing genetic diversity to buffer against inbreeding depression and to boost diversifying selection (Bakker et al., 2009; Meimberg et al., 2009). The environmental success of the young colonizers of *B. hybridum* in the Americas, southern Africa, and Oceania might also be related to rapid shifts in physiological and adaptive traits, such as changes in flowering time related to photoperiod and weediness (cf. Bakker et al., 2009). Yet the underlying factors causing the apparent different adaptive capabilities of *B. hybridum* in its native range and in the allochthonous areas should be tested through more detailed studies. It would also require the corroboration of the apparent but still unconfirmed absence of the diploid *B. distachyon* and *B. stacei* parents in those areas.

ACKNOWLEDGEMENTS

The authors thanks R. Jaime (Univ. Jaén) and D. Draper (Univ. Loja) for fruitful discussion on ENM analysis, and several colleagues (listed in Appendix S1) and the RNG (Reading), M (Munich), and SALA (Salamanca) herbaria for providing us with georeferenced *B. distachyon*, *B. stacei*, and *B. hybridum* samples. The study has been funded by two consecutive Spanish Ministry of Science grant projects (CGL2009-12955-C02-01, CGL2012-39953-C02-01) and an Aragon Government and European Social Fund Bioflora grant to P.C. and D.L.-A; D.L.-A. was funded by a Spanish Ministry of Science FPI fellowship.

LITERATURE CITED

Anderson, R. P., A. T. Peterson, and M. Gomez-Laverde. 2002. Using niche-based GIS modeling to test geographic predictions of competitive exclusion and competitive release in South American pocket mice. *Oikos* 98: 3–16.

Araujo, M. B., and C. Rahbek. 2006. How does climate change affect biodiversity? *Science* 313: 1396–1397.

Atwell, B. J., P. E. Kriedemann, and C. G. N. Turnbull, and Australian Society of Plant Physiologists. 1999. Plants in action: Adaptation in nature, performance in cultivation. MacMillan Education Australia, South Yarra (Australia).

Austin, M. P., and T. M. Smith. 1989. A new model for the continuum concept. *Vegetatio* 83: 35–47.

Bakker, E. G., B. Montgomery, T. Nguyen, K. Eide, J. Chang, T. C. Mockler, A. Liston, et al. 2009. Strong population structure characterizes weediness gene evolution in the invasive grass species *Brachypodium distachyon*. *Molecular Ecology* 18: 2588–2601.

Banks, W. E., F. d'Errico, A. T. Peterson, M. Kageyama, and G. Colombeau. 2008. Reconstructing ecological niches and geographic distributions of caribou (*Rangifer tarandus*) and red deer (*Cervus elaphus*) during the Last Glacial Maximum. *Quaternary Science Reviews* 27: 2568–2575.

Benito, B. M., M. M. Martínez-Ortega, L. M. Muñoz, J. Lorite, and J. Peñas. 2009. Assessing extinction-risk of endangered plants using species distribution models: A case study of habitat depletion caused by the spread of greenhouses. *Biodiversity and Conservation* 18: 2509–2520.

Boria, R. A., L. E. Olson, S. M. Goodman, and R. P. Anderson. 2014. Spatial filtering to reduce sampling bias can improve the performance of ecological niche models. *Ecological Modelling* 275: 73–77.

Brown, J. H. 1984. On the relationship between abundance and distribution of species. *American Naturalist* 124: 255–279.

Brown, J. L. 2014. SDMtoolbox: A python-based GIS toolkit for landscape genetic, biogeographic and species distribution model analyses. *Methods in Ecology and Evolution* 5: 694–700.

Buggs, R. J. A., and J. R. Pannell. 2007. Ecological differentiation and diploid superiority across a moving ploidy contact zone. *Evolution* 61: 125–140.

Catalán, P., B. Chalhoub, V. Chochois, D. F. Garvin, R. Hasterok, A. J. Manzaneda, L. A. J. Mur, et al. 2014. Update on the genomics and basic biology of International *Brachypodium* Initiative (IBI). *Trends in Plant Science* 19: 414–418.

Catalán, P., J. Muller, R. Hasterok, G. Jenkins, L. A. J. Mur, T. Langdon, A. Betekhtin, et al. 2012. Evolution and taxonomic split of the model grass *Brachypodium distachyon*. *Annals of Botany* 109: 385–405.

Clark, P. U., and A. C. Mix. 2002. Ice sheets and sea level of the Last Glacial Maximum. *Quaternary Science Reviews* 21: 1–7.

Collins, W. D., C. M. Bitz, M. L. Blackmon, G. B. Bonan, C. S. Bretherton, J. A. Carton, P. Chang, et al. 2006. The Community Climate System Model version 3 (CCSM3). *Journal of Climate* 19: 2122–2143.

Elith, J., C. H. Graham, R. P. Anderson, M. Dudik, S. Ferrier, A. Guisan, R. J. Hijmans, et al. 2006. Novel methods improve prediction of species' distributions from occurrence data. *Ecography* 29: 129–151.

Elith, J., M. Kearney, and S. Phillips. 2010. The art of modelling range-shifting species. *Methods in Ecology and Evolution* 1: 330–342.

Estep, M. C., M. R. McKain, D. V. Diaz, J. S. Zhong, J. G. Hodge, T. R. Hodkinson, D. J. Layton, et al. 2014. Allopolyploidy, diversification, and the Miocene grassland expansion. *Proceedings of the National Academy of Sciences, USA* 111: 15149–15154.

Evans, M. E. K., S. A. Smith, R. S. Flynn, and M. J. Donoghue. 2009. Climate, niche evolution, and diversification of the "bird-cage" evening primroses (*Oenothera*, sections *Anogra* and *Kleinia*). *American Naturalist* 173: 225–240.

Feliner, G. N. 2011. Southern European glacial refugia: A tale of tales. *Taxon* 60: 365–372.

Fernández-Mazuecos, M., and P. Vargas. 2013. Congruence between distribution modelling and phylogeographical analyses reveals Quaternary survival of a toadflax species (*Linaria elegans*) in oceanic climate areas of a mountain ring range. *New Phytologist* 198: 1274–1289.

Garvin, D. F., Y. Q. Gu, R. Hasterok, S. P. Hazen, G. Jenkins, T. C. Mockler, L. A. J. Mur, and J. P. Vogel. 2008. Development of genetic and genomic

research resources for *Brachypodium distachyon*, a new model system for grass crop research. *Crop Science* 48: S69–S84.

Geber, M. A., and L. R. Griffen. 2003. Inheritance and natural selection on functional traits. *International Journal of Plant Sciences* 164: S21–S42.

Giraldo, P., M. Rodríguez-Quijano, J. F. Vázquez, J. M. Carrillo, and E. Benavente. 2012. Validation of microsatellite markers for cytotype discrimination in the model grass *Brachypodium distachyon*. *Genome* 55: 523–527.

Godsoe, W., M. A. Larson, K. L. Glennon, and K. A. Segraves. 2013. Polyploidization in *Heuchera cylindrica* (Saxifragaceae) did not result in a shift in climatic requirements. *American Journal of Botany* 100: 496–508.

Gordon, S. P., H. Priest, D. L. D. Marais, W. Schackwitz, M. Figueroa, J. Martin, J. N. Bragg, et al. 2014. Genome diversity in *Brachypodium distachyon*: Deep sequencing of highly diverse inbred lines. *Plant Journal* 79: 361–374.

Graham, C. H., S. R. Ron, J. C. Santos, C. J. Schneider, and C. Moritz. 2004. Integrating phylogenetics and environmental niche models to explore speciation mechanisms in dendrobatid frogs. *Evolution* 58: 1781–1793.

Green, R. H. 1971. Multivariate statistical approach to the Hutchinsonian niche: bivalve molluscs of Central Canada. *Ecology* 52: 543.

Hammer, Ø., D. A. T. Harper, and P. D. Ryan. 2001. PAST: Paleontological statistics software package for education and data analysis. *Palaeontologia Electronica* 4: 9.

Hernandez, P. A., C. H. Graham, L. L. Master, and D. L. Albert. 2006. The effect of sample size and species characteristics on performance of different species distribution modeling methods. *Ecography* 29: 773–785.

Hewitt, G. M. 2004. Genetic consequences of climatic oscillations in the Quaternary. *Philosophical Transactions of the Royal Society of London, B, Biological Sciences* 359: 183–195.

Hijmans, R., L. Guarino, P. Mathur, and A. Jarvis. 2005a. DIVA-GIS [online computer program]. Available at http://www.diva-gis.org/.

Hijmans, R. J., S. E. Cameron, J. L. Parra, P. G. Jones, and A. Jarvis. 2005b. Very high resolution interpolated climate surfaces for global land areas. *International Journal of Climatology* 25: 1965–1978.

Hutchinson, G. E. 1957. Concluding remarks. In Population studies: Animal ecology and demography. *Cold Spring Harbor Symposia on Quantitative Biology* 22: 415–427.

Jaime, R., J. M. Alcántara, J. M. Bastida, and P. J. Rey. 2015. Complex patterns of environmental niche evolution Iberian columbines (gen. *Aquilegia*, Ranunculaceae). *J Plant Ecology*.

Jenkins, G., R. Hasterok, and J. Draper. 2003. Building the molecular infrastructure of a new model grass. *In* Z. Zwierzykowski, M. Surma, and P. Kachlicki [eds.], Application of novel cytogenetic and molecular techniques in genetics and breeding of the grasses, 77–84. Institute of Plant Genetics of the Polish Academy of Sciences, Poznan, Poland.

Johnson, M. T. J., B. C. Husband, and T. L. Burton. 2003. Habitat differentiation between diploid and tetraploid *Galax urceolata* (Diapensiaceae). *International Journal of Plant Sciences* 164: 703–710.

K-1 Model Developers. 2004. K-1 coupled GCM (MIROC) description. K-1 Technical Report No. 1, Center for Climate Research, University of Tokyo, Tokyo, Japan.

Kirkpatrick, M., and N. H. Barton. 1997. Evolution of a species' range. *American Naturalist* 150: 1–23.

Kozak, K. H., C. H. Graham, and J. J. Wiens. 2008. Integrating GIS-based environmental data into evolutionary biology. *Trends in Ecology & Evolution* 23: 141–148.

Lambeck, K., and J. Chappell. 2001. Sea level change through the last glacial cycle. *Science* 292: 679–686.

Lambeck, K., Y. Yokoyama, and T. Purcell. 2002. Into and out of the Last Glacial Maximum: Sea-level change during oxygen isotope stages 3 and 2. *Quaternary Science Reviews* 21: 343–360.

Levin, D. A. 1975. Minority cytotype exclusion in local plant populations. *Taxon* 24: 35–43.

Levin, D. A. 1983. Polyploidy and novelty in flowering plants. *American Naturalist* 122: 1–25.

López-Alvarez, D., M. L. López-Herranz, A. Betekhtin, and P. Catalan. 2012. A DNA barcoding method to discriminate between the model plant *Brachypodium distachyon* and its close relatives *B. stacei* and *B. hybridum* (Poaceae). *PLoS ONE* 7: e51058.

Mandle, L., D. L. Warren, M. H. Hoffmann, A. T. Peterson, J. Schmitt, and E. J. von Wettberg. 2010. Conclusions about niche expansion in introduced *Impatiens walleriana* populations depend on method of analysis. *PLoS ONE* 5(12): e15297.

Manzaneda, A. J., P. J. Rey, J. M. Bastida, C. Weiss-Lehman, E. Raskin, and T. Mitchell-Olds. 2012. Environmental aridity is associated with cytotype segregation and polyploidy occurrence in *Brachypodium distachyon* (Poaceae). *New Phytologist* 193: 797–805.

Martin, S. L., and B. C. Husband. 2009. Influence of phylogeny and ploidy on species ranges of North American angiosperms. *Journal of Ecology* 97: 913–922.

McCormack, J. E., A. J. Zellmer, and L. L. Knowles. 2010. Does niche divergence accompany allopatric divergence in Aphelocoma jays as predicted under ecological speciation?: Insights from tests with niche models. *Evolution* 64: 1231–1244.

McIntyre, P. J. 2012. Polyploidy associated with altered and broader ecological niches in the *Claytonia perfoliata* (Portulacaceae) species complex. *American Journal of Botany* 99: 655–662.

Médail, F., and K. Diadema. 2009. Glacial refugia influence plant diversity patterns in the Mediterranean Basin. *Journal of Biogeography* 36: 1333–1345.

Meimberg, H., K. J. Rice, N. F. Milan, C. C. Njoku, and J. K. McKay. 2009. Multiple origins promote the ecological amplitude of allopolyploid *Aegilops* (Poaceae). *American Journal of Botany* 96: 1262–1273.

Meyers, L. A., and D. A. Levin. 2006. On the abundance of polyploids in flowering plants. *Evolution* 60: 1198–1206.

Miller, J., and J. Franklin. 2002. Modeling the distribution of four vegetation alliances using generalized linear models and classification trees with spatial dependence. *Ecological Modelling* 157: 227–247.

Mur, L. A. J., J. Allainguillaume, P. Catalan, R. Hasterok, G. Jenkins, K. Lesniewska, I. Thomas, and J. Vogel. 2011. Exploiting the *Brachypodium* Tool Box in cereal and grass research. *New Phytologist* 191: 334–347.

Nakazato, T., D. L. Warren, and L. C. Moyle. 2010. Ecological and geographic modes of species divergence in wild tomatoes. *American Journal of Botany* 97: 680–693.

Oliver, J. L., and M. Ruiz-Rejon. 1980. Relation between isozymes and ploidy level. Its application to biogeographical studies of *Muscari atlanticum* (Liliaceae). *Taxon* 29: 27–32.

Ortega-Huerta, M. A., and A. T. Peterson. 2008. Modeling ecological niches and predicting geographic distributions: A test of six presence-only methods. *Revista Mexicana de Biodiversidad* 79: 205–216.

Otto-Bliesner, B. L., S. J. Marsha, J. T. Overpeck, G. H. Miller, A. X. Hu, and C. L. I. P. Mem. 2006. Simulating arctic climate warmth and icefield retreat in the last interglaciation. *Science* 311: 1751–1753.

Pandit, M. K., M. J. O. Pocock, and W. E. Kunin. 2011. Ploidy influences rarity and invasiveness in plants. *Journal of Ecology* 99: 1108–1115.

Pearson, R. G., C. J. Raxworthy, M. Nakamura, and A. T. Peterson. 2007. Predicting species distributions from small numbers of occurrence records: A test case using cryptic geckos in Madagascar. *Journal of Biogeography* 34: 102–117.

Peterson, A. T. 2011. Ecological niche conservatism: A time-structured review of evidence. *Journal of Biogeography* 38: 817–827.

Peterson, A. T., and R. D. Holt. 2003. Niche differentiation in Mexican birds: Using point occurrences to detect ecological innovation. *Ecology Letters* 6: 774–782.

Peterson, A. T., and A. S. Nyari. 2008. Ecological niche conservatism and pleistocene refugia in the thrush-like mourner, *Schiffornis* sp., in the neotropics. *Evolution* 62: 173–183.

Peterson, A. T., M. Papes, and M. Eaton. 2007. Transferability and model evaluation in ecological niche modeling: A comparison of GARP and Maxent. *Ecography* 30: 550–560.

Peterson, A. T., J. Soberon, and V. Sánchez-Cordero. 1999. Conservatism of ecological niches in evolutionary time. *Science* 285: 1265–1267.

Phillips, S. J., R. P. Anderson, and R. E. Schapire. 2006. Maximum entropy modeling of species geographic distributions. *Ecological Modelling* 190: 231–259.

Raes, N., M. C. Roos, J. W. F. Slik, E. E. van Loon, and H. ter Steege. 2009. Botanical richness and endemicity patterns of Borneo derived from species distribution models. *Ecography* 32: 180–192.

Raxworthy, C. J., C. M. Ingram, N. Rabibisoa, and R. G. Pearson. 2007. Applications of ecological niche modeling for species delimitation: A review and empirical evaluation using day geckos (*Phelsuma*) from Madagascar. *Systematic Biology* 56: 907–923.

Rundell, R. J., and T. D. Price. 2009. Adaptive radiation, nonadaptive radiation, Ecological speciation and nonecological speciation. *Trends in Ecology & Evolution* 24: 394–399.

Russell, J., M. van Zonneveld, I. K. Dawson, A. Booth, R. Waugh, and B. Steffenson. 2014. Genetic diversity and ecological niche modelling of wild barley: Refugia, large-scale post-LGM range expansion and limited mid-future climate threats? *PLoS ONE* 9(2): e86021.

Schippmann, U. 1991. Revision der europäischen Arten der Gattung *Brachypodium* Palisot de Beauvois (Poaceae), vol. 45. Conservatoire et Jardin Botaniques de Genève, Geneva, Switzerland.

Schoener, T. W. 1968. The *Anolis* lizards of Bimini—Resource partitioning in a complex fauna. *Ecology* 49: 704.

Smith, S. A., and M. J. Donoghue. 2010. Combining historical biogeography with niche modeling in the *Caprifolium* clade of *Lonicera* (Caprifoliaceae, Dipsacales). *Systematic Biology* 59: 322–341.

Soberón, J. M. 2010. Niche and area of distribution modeling: A population ecology perspective. *Ecography* 33: 159–167.

Soltis, D. E., and P. S. Soltis. 1999. Polyploidy: Recurrent formation and genome evolution. *Trends in Ecology & Evolution* 14: 348–352.

Stebbins, G. L. 1971. Chromosomal evolution in higher plants. Edward Arnold, London, UK.

Stevens, B., M. Giorgetta, M. Esch, T. Mauritsen, T. Crueger, S. Rast, M. Salzmann, et al. 2013. Atmospheric component of the MPI-M Earth System Model: ECHAM6. *Journal of Advances in Modeling Earth Systems* 5: 146–172.

Stewart, J. R., A. M. Lister, I. Barnes, and L. Dalen. 2010. Refugia revisited: Individualistic responses of species in space and time. *Proceedings of the Royal Society, B, Biological Sciences* 277: 661–671.

Tarkhnishvili, D., A. Gavashelishvili, and L. Mumladze. 2012. Palaeoclimatic models help to understand current distribution of Caucasian forest species. *Biological Journal of the Linnean Society* 105: 231–248.

te Beest, M., J. J. Le Roux, D. M. Richardson, A. K. Brysting, J. Suda, M. Kubesova, and P. Pysek. 2012. The more the better? The role of polyploidy in facilitating plant invasions. *Annals of Botany* 109: 19–45.

Vogel, J. P., D. F. Garvin, T. C. Mockler, J. Schmutz, D. Rokhsar, M. W. Bevan, K. Barry, et al. 2010. Genome sequencing and analysis of the model grass *Brachypodium distachyon*. *Nature* 463: 763–768.

Vogel, J. P., M. Tuna, H. Budak, N. X. Huo, Y. Q. Gu, and M. A. Steinwand. 2009. Development of SSR markers and analysis of diversity in Turkish populations of *Brachypodium distachyon*. *BMC Plant Biology* 9: 88.

Waltari, E., R. J. Hijmans, A. T. Peterson, A. S. Nyari, S. L. Perkins, and R. P. Guralnick. 2007. Locating Pleistocene eefugia: Comparing phylogeographic and ecological niche model predictions. *PLoS ONE* 2(7): e563.

Warren, D. L., R. E. Glor, and M. Turelli. 2008. Environmental niche equivalency versus conservatism: Quantitative approaches to niche evolution. *Evolution* 62: 2868–2883.

Warren, D. L., R. E. Glor, and M. Turelli. 2010. ENMTools: A toolbox for comparative studies of environmental niche models. *Ecography* 33: 607–611.

Wiens, J. J., and C. H. Graham. 2005. Niche conservatism: Integrating evolution, ecology, and conservation biology. *Annual Review of Ecology, Evolution and Systematics* 36: 519–539.

Wisz, M. S., R. J. Hijmans, J. Li, A. T. Peterson, C. H. Graham, A. Guisan, and N. P. S. Distribut. 2008. Effects of sample size on the performance of species distribution models. *Diversity & Distributions* 14: 763–773.

Wollan, A. K., V. Bakkestuen, H. Kauserud, G. Gulden, and R. Halvorsen. 2008. Modelling and predicting fungal distribution patterns using herbarium data. *Journal of Biogeography* 35: 2298–2310.

Woodward, F. I. 1988. Climate and plant distribution, reprinted ed. Cambridge University Press, Cambridge, UK.